Electronic Supplementary Information

Non-excitonic defect-assisted radiative transitions are responsible for new D-type blinking in ternary quantum dots

Adam Olejniczak[1], Ryan Rich[2], Zygmunt Gryczynski[3] and Bartłomiej Cichy[1]*

[1] Institute of Low Temperature and Structure Research, Polish Academy of Sciences, Okólna 2, 50-422 Wrocław, Poland

[2] Department of Mathematics, Computer Science and Physics, Texas Wesleyan University, 1201 Wesleyan Street, Fort Worth, TX 76105, USA

[3] Department of Physics and Astronomy, Texas Christian University, Fort Worth, TX 76129, USA

*corresponding author: b.cichy@intibs.pl

Section 1. Synthesis procedure of $AgInS_2$ and $CuInS_2$ quantum dots

All of the quantum dots (QDs) were synthesized using the wet chemical route. Copper-indium disulfide ($CuInS_2$, CIS) QDs were synthesized by a thermal decomposition method. The synthesis procedure was performed in 1-octadecene (ODE) used as a solvent. Copper(I) iodide (CuI) and indium(III) acetate $In(OAc)_3$ were used as the reagents along with 1-dodecanethiol (DDT) used as the stabilizing ligand as well as the sulfur source. The reaction was performed under reduced pressure (c.a. 8 hPa) at 140°C degrees. Finally, the CIS QDs were dispersed in chloroform ($CHCl_3$). The silver-indium disulfide ($AgInS_2$, AIS) QDs were synthesized via metathesis reaction between metal thiolates and sulfur source. Indium(III) acetate ($In(OAc)_3$, 99.99%), silver nitrate ($AgNO_3$, 99.9%), 1-dodecanethiol (DDT, 98%) and sublimated sulfur (S, 99%) were used in the synthesis. At first a mixture of $AgNO_3$, $In(OAc)_3$ metal salts and DDT was preheated and degassed at 60ºC for 30 minutes. Sulfur precursor was prepared by dissolving of sublimated sulfur in 3 cm^3 DDT. After thiolates formation at 110ºC the sulfur precursor was swiftly injected into the mixture, starting the AIS QDs synthesis. Final product was also dispersed in chloroform.

Section 2. Single-particle measurements details

Photoluminescence traces from individual $CuInS_2$ and $AginS_2$ QDs were taken using the PicoQuant MicroTime 200 confocal fluorescence system. The 470 nm (PicoQuant) picosecond laser diode operating at 1 MHz was used as the excitation source in the experiments. The silicon single-photon avalanche Perkin Elmer (SPCM-AQR-14) photodiode was used as the detector. Scattered light was removed by a 473 nm interference long pass filter. The time-tagged time-resolved (TTTR) mode of single photon events collection was used in the measurements. All data processing of the TTTR data sets was performed by self-written custom algorithms.

Section 3. Additional single particle measurements results

Additional results for individual $CuInS_2$ quantum dots

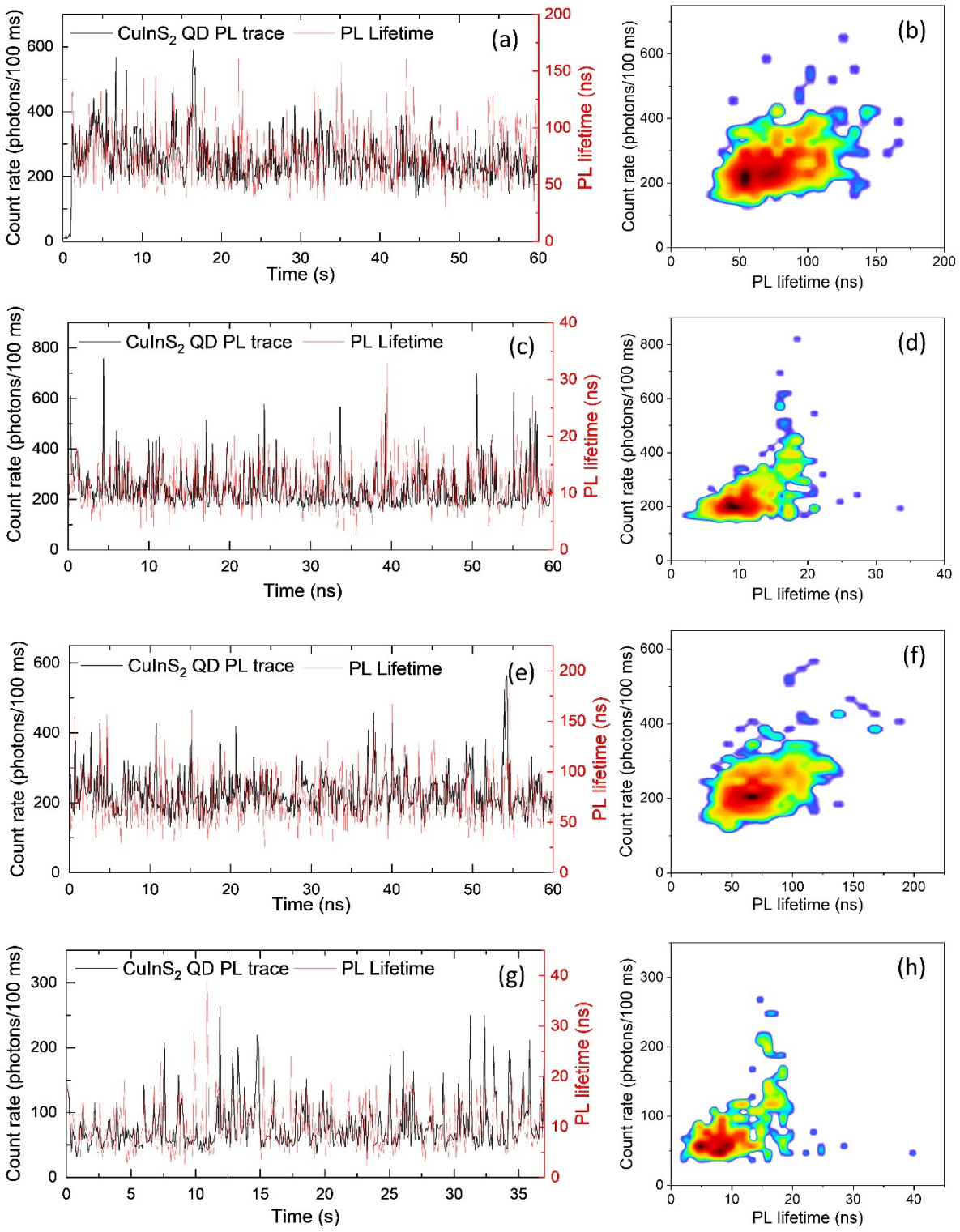

Figure S1. (a, c, e, g) Photoluminescence (black) and lifetime (red) traces calculated for 100 ms bins and (b, d, f, h) corresponding FLID maps of individual $CuInS_2$ QDs.

Additional results for individual $AgInS_2$ quantum dots

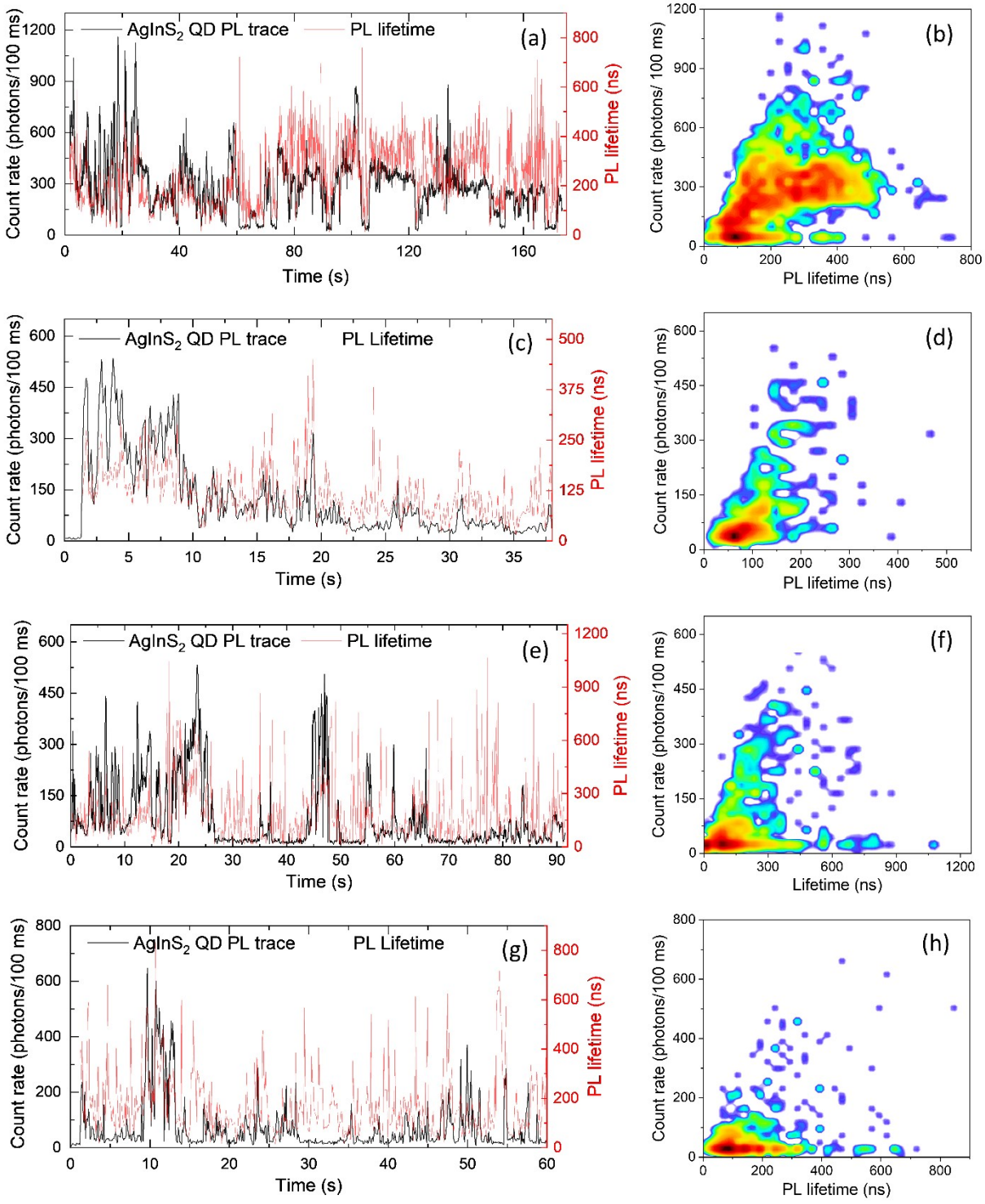

Figure S2. (a, c, e, g) Photoluminescence (black) and lifetime (red) traces calculated for 100 ms bins and (b, d, f, h) corresponding FLID maps of individual $AgInS_2$ QDs.

Section 4. Kinetic Monte Carlo calculation details

Simulation of kinetic processes occurring in single I-III-VI QD was performed numerically within the Kinetic Monte Carlo (KMC) method[1,2]. To avoid unnecessary complication in the simulation procedure, an arbitrary QD is considered as a simple two-level system, i.e. ground and excited state, with an additional trap state that can bind excited carriers and provide a nonradiative relaxation path. Such simplification is justified by the fact that formation of the dark state requires defects assisted relaxation. Note that we do not take the electron spin or Pauli exclusion principle into consideration. In the case of three or more excited electrons, all will be in the same excited state. Processes involving higher excited states are omitted in the current discussion. From a numerical point of view, trapping rates of excited electrons or holes can be arbitrary chosen, and physical constants (effective mass, carrier concentration, defect states ionization energy etc.) were neglected in the first approximation. For the same processes and their rates considered either for electrons or holes, analogous results would be obtained. Hence calculation for just one carrier type may be done without losing of the problem generality. For this reason, all simulations were performed only for electrons. It is however important to note that real-life transitions of excited electrons or holes to the respective donor/acceptor trapping centres in semiconductors will be characterized by different transition rates, depending on carrier effective mass, trap state location in the forbidden region or temperature. Trapping or detrapping rates would also differ for surface defects and deep or shallow states inside the bandgap. Here we do not take into the consideration the physical nature of the trap, which is completely defined only by its rate constants. Electronic transition probabilities are described by corresponding rate equations. The rates were parameterized by rate constants $k_n = 1/\tau_n$, where τ_n is associated with the lifetime constant. Time constant τ_n is then the average time spent in some QD state before event "n" occur. For example, trapping time constant (τ_t) is the average time that passes before excited electron is transferred to a trap state. Time constant of radiative recombination from a trap state (τ_{rt}) is the actual time that electron spends in a trap state before it can emit. Henceforth we will use the time constant τ_n rather than k_n to describe the process rate.

Three different models covering the problems of radiative recombination from a single trap centre (M1), trapping of more than one electron by a single defect site resulting in the change of its charge state (M2) and the interplay of two different (radiative and non-radiative) defect levels (M3) were considered in this work. All of the processes enclosed in these models may be considered as the most probable for the I-III-VI system. Conventional charging model was calculated first as a reference for further discussion.

Conventional charging model

Charging model was historically first model of QDs blinking proposed by Efros and Rosen[3]. They assumed that after creation of two electron-hole pairs, one electron can be photoionized after nonradiative Auger recombination of second electron-hole pair. Photoionized electron is transferred to external long-living trap state related to surface state or surrounding matrix. QD core is now positively charged by remaining hole, which can effectively quench luminescence by nonradiative Auger processes. This mechanism is often referred as A-type blinking. In our work, we have simulated charging model as described by Ye and Searson[4]. The notation, set of optical processes and rate equations described there were followed here. Any possible QD state is here unambiguously described by a set of two indices (i,j), where i stands for the total number of excited electron-hole pairs and j denotes the number of electrons transferred to a trap state. Further, the number of occupied trap states is specified by s^-. According to this notation scheme, one may notice that hole and electron concentrations are $p = i$, $n = i - j$ respectively, and the number of trapped electrons is $s^- = j$.

The following electronic transitions are considered over all of the schemes (**fig. S3**): (i) generation – g – describing probability of electron-hole pair generation, (ii) radiative relaxation r, (iii) electron transfer to an empty trap t, (iv) electron detrapping dt and (v) non-radiative trapped electron-hole relaxation nrt, and (vi) three-particle non-radiative recombination by Auger process – A.

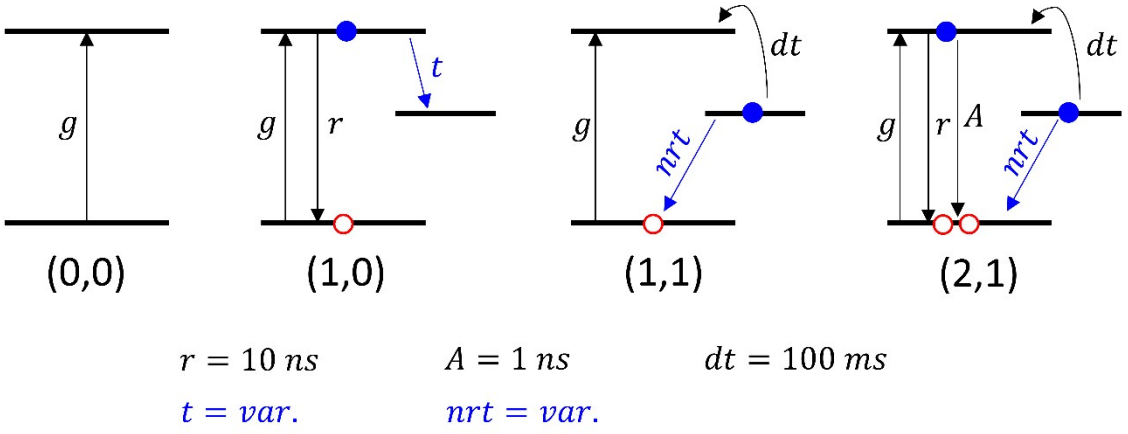

Figure S3. Simplified flow chart of optical processes considered in simulation of conventional charging model. Rate constants common for all calculations: $\tau_r = 10\ ns$, $\tau_{dt} = 100\ ms$, $\tau_A = 1\ ns$ are coloured in black. Rates varied in calculations are coloured in blue. Filled blue circles represent electrons, while open red circles represent holes. The (i, j) indexing convention is shown for each state in parentheses.

Table S1. Rate equations for processes included in conventional charging model calculations.

Process	Shortcut	Rate equation
Generation	g	$\frac{I \cdot \sigma}{E_{ph}}$
Exciton radiative recombination	r	$k_r \cdot n \cdot p$
Charge trapping	t	$k_t \cdot n \cdot s^0$
Charge detrapping	dt	$k_{dt} \cdot s^-$
Nonradiative recombination from trap state	nrt	$k_{nrt} \cdot s^- \cdot p$
Auger nonradiative recombination	A	$k_A \cdot n \cdot p^2$

Rate equations of processes considered in charging model are gathered in **tab. S1**. Generation is allowed at any state of the QD. Excitation parameters were chosen here as follows: excitation intensity: $I = 160 W/cm^2$, absorption cross section $\sigma = 5 \cdot 10^{-16}\ cm^2$, and excitation photon energy $E_{exc} = 2.5\ eV$. These values are common for generation in every calculated model. The total number of traps was arbitrarily chosen as $s = s^0 + s^- = 10$. Every trap can be filled with only one electron. It was assumed that the trap state is located energetically lower than the excited state. Therefore, transitioning back to the excited state after a trapping event should be of low probability. In the real world this may be a result of tunnelling, photon absorption, scattering or energy transfer from Auger processes. Hence the detrapping rate was fixed to $\tau_{dt} = 100\ ms$. The rate of radiative recombination of the electron-hole pair was fixed for all simulations. The value for τ_r was chosen to be $\tau_r = 10\ ns$, which is in order of magnitude typical for most semiconductor nanocrystals. The Auger rate constant was set to be an

order of magnitude faster than radiative exciton recombination, $\tau_A = 1\ ns$, but values on the order of hundreds of picoseconds are also reported in the literature[5]. The KMC simulations were carried out for a total time of at least 5 seconds, being long enough to obtain proper statistics for every possible optical process. Photons emitted during the simulation steps were binned to 10 ms intervals and plotted as photoluminescence traces. For every emitted photon, the incoming time was ascribed as a time interval between previous generation event and following emission event. Within every 10 ms interval, the photon incoming times were gathered into the histogram and fitted using the first-order decay law. According to fluorescence lifetime-intensity distribution (FLID) maps, each 10 ms interval is associated with a set of two numbers – intensity of emission and photoluminescence lifetime – (I_{ems},τ_{PL}). The colouring represents then the probability of finding an interval during the simulation with given I_{ems} and τ_{PL}. Colour scale on every FLID maps is white(zero)-blue-cyan-green-yellow-orange-red(max).

In the first place, calculations within charging model were performed for a wide range of trapping rates $\tau_t = (10\ ns, 100\ ns, 1\ \mu s, 10\ \mu s, 100\ \mu s, 1\ ms, 10\ ms, 100\ ms)$ with fixed long-lasting stay of electron in a trap ($\tau_{nrt} = 100\ ms$). Next, the same wide range ($10\ ns - 100\ ms$) was adopted to τ_{nrt} with fixed trapping rate $\tau_t = 1\ ms$. These two sets of calculations were then repeated for a faster nonradiative decay rate ($\tau_{nrt} = 1\ ms$) and a trapping rate ($\tau_t = 1\ \mu s$) respectively.

Model M1

Model M1 was the first attempt to mimic optical processes characteristic for ternary semiconductor QDs by opening a pathway for radiative relaxation from a trap centre. All transitions considered previously in conventional charging model were considered also in model M1 (**fig. S4**). The additional rate equation for radiative recombination from a trap was analogous to the rate equation for nonradiative recombination (**tab. S2**).

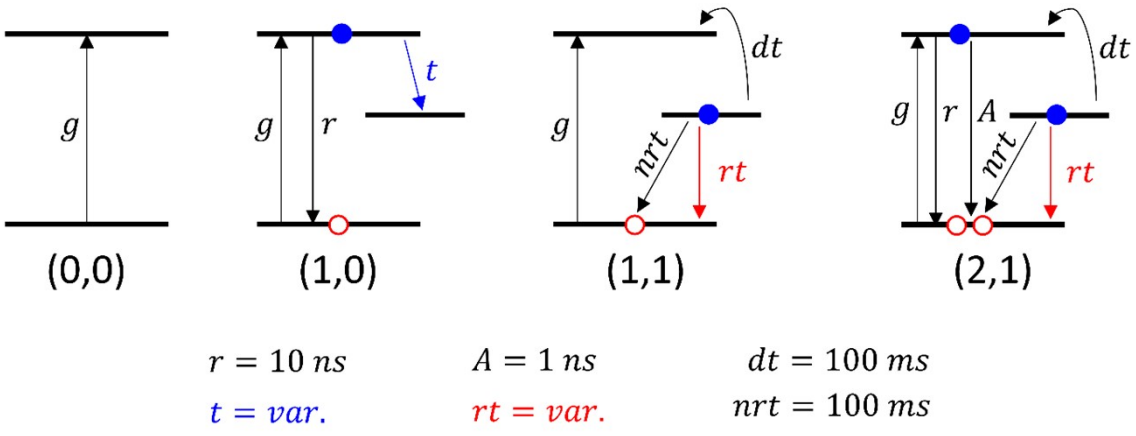

Figure S4. Simplified flow chart of optical processes considered in simulation of **M1** model. Rate constants common for all calculations: $\tau_r = 10\ ns$, $\tau_{dt} = \tau_{nrt} = 100\ ms$, $\tau_A = 1\ ns$ are coloured in black. Rates varied in calculations are coloured in blue and red. Filled blue circles represent electrons, while open red circles represent holes. The (i, j) indexing convention as shown in parentheses is the same as in charging model.

Table S2. Rate equation used in model M1 in addition to all rate equations for conventional charging model (**tab. S1**).

Process	Shortcut	Rate equation
Radiative recombination from trap state	rt	$k_{rt} \cdot s^{-} \cdot p$

First, the wide range of $\tau_{rt} \in (10\ ns - 100\ ms)$ were simulated with fixed values of trapping and nonradiative recombination rates ($\tau_t = 1\ ms$ and $\tau_{nrt} = 100\ ms$) to find the influence of trap state radiative recombination on type-A blinking behaviour. Next, faster trappings and radiative recombination from traps were considered in pairs (τ_t, τ_{rt}), where $\tau_t \in (10\ ns, 100\ ns, 1\ \mu s)$ and $\tau_{rt} \in (10\ ns, 100\ ns, 1\ \mu s, 10\ \mu s)$. Photons emitted during exciton (r) and trap state (rt) radiative recombination were always distinguished during the analysis of the results. However, since the defect level in our model is not assigned to any specific point defect, we do not define the energy of the photon emitted from trap state radiative recombination. Separate photoluminescence traces and FLID maps were plotted for both radiative recombination channels as well as for their sum as the total emission.

Model M2

The second model is devoted to hypothetical defect states that may be populated by more than one electron. It is used to describe temporal fluctuation for trapped electron relaxation rates and switching between emissive and non-emissive behaviour of a trap centre. This model was formulated in analogy to defect centres formed by native point defects and defect clusters existing in the group of I-III-VI compounds. Change in a charge state, i.e. from singly to doubly charged defect (-/2-), is therefore responsible for the energy shift of this level. By changing the charge state, one may also change the character of the electronic transitions occurring from it.

In this scheme, it was allowed for every occupied defect level to trap more than one electron. Here we assume that a maximum of two electrons can be trapped in single defect level. Only one charge state can lead to radiative relaxations. It was also assumed that the position of double occupied defect state will shift in the energy gap between the conduction and valence bands, and therefore the rate of detrapping events will differ from that of a single occupied defect state. The exact value of the shift in the energy level is not considered, however photons emitted from doubly-occupied traps are distinguished from other emission sources during analysis of the simulation results. All processes considered in M2 model was schematically presented in **fig. S5**.

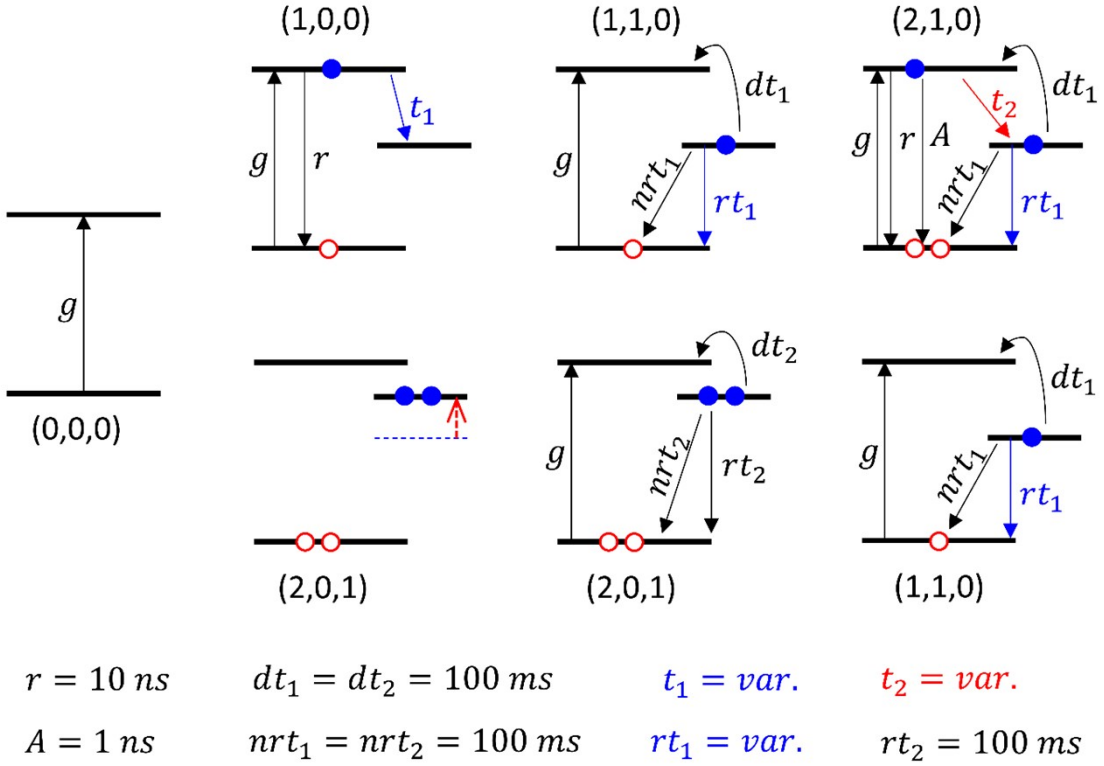

Figure S5. Simplified flow chart of electronic transitions comprised by model **M2.** This model encompasses change in the transition rate due to the single (subscript **1**) or double (subscript **2**) occupation of a trap state. Rates common for all calculations: $\tau_r = 10\ ns$, $\tau_A = 1\ ns$, $\tau_{dt1} = \tau_{dt2} = 100\ ms$, $\tau_{nrt1} = \tau_{nrt2} = 100\ ms$, $\tau_{rt2} = 100\ ms$ were noted in black. Rates varied in calculations were noted in blue and red. Filled blue circles represent electrons, while open red circles represent holes. The (i,j,k) indexing convention is shown for each state in parentheses.

In contrast to the scheme **M1** in this model, the QD state is described by a set of three parameters (i,j,k), where i is the total number of excited electron-hole pairs, j is the number of single occupied traps and k is the number of double occupied traps. We define $p = i$ and $n = i - j - 2k$ as the number of free holes and free electrons respectively. $s^- = j$ and $s^{2-} = k$ are the number of single and double occupied traps respectively. The total number of traps was $s = s^0 + s^- + s^{2-} = 10$. Since trapping of two electrons occurs one after the other, the number of single occupied traps s^- is at the same time the possible number of traps that can change their charge state. Transitions to/from single occupied traps are named with subscript **1**, while transitions to/from doubly occupied traps are named with subscript **2**. Rate equations for transitions including double occupied states are given in **tab. S3**. We set detrapping time constants to $\tau_{dt1} = \tau_{dt2} = 100\ ms$ which is equal to nonradiative decay time constants $\tau_{nrt1} = \tau_{nrt2} = 100\ ms$. The radiative recombination time constant for the double occupied defect level was fixed at $\tau_{rt2} = 100\ ms$ to ensure its non-radiative character. Rates for generation, radiative and Auger recombination were the same as in model **M1**. All abovementioned rates were common and fixed for all calculations done within this model.

Table S3. Rate equations for processes included in model M2.

Process		Shortcut	Rate equation
Generation		g	$\frac{I \cdot \sigma}{E_{ph}}$
Exciton radiative recombination		r	$k_r \cdot n \cdot p$
Charge trapping	First charge carrier	t_1	$k_{t1} \cdot n \cdot s^0$
	Second charge carrier	t_2	$k_{t2} \cdot n \cdot s^-$
Charge detrapping	Single-occupied trap	dt_1	$k_{dt1} \cdot s^-$
	Double-occupied trap	dt_2	$k_{dt2} \cdot 2 \cdot s^{2-}$
Nonradiative recombination from trap state	Single-occupied trap	nrt_1	$k_{nrt1} \cdot s^- \cdot p$
	Double-occupied trap	nrt_2	$k_{nrt2} \cdot 2 \cdot s^{2-} \cdot p$
Radiative recombination from trap state	Single-occupied trap	rt_1	$k_{rt1} \cdot s^- \cdot p$
	Double-occupied trap	rt_2	$k_{rt2} \cdot 2 \cdot s^{2-} \cdot p$
Auger		A	$k_A \cdot n \cdot p^2$

The influence of switching between emissive and non-emissive character of trap states on the photoluminescence is governed by the interplay of three parameters: single trap population rate τ_{t1}, radiative recombination of trapped electron τ_{rt1} and switching to nonradiative state by second electron trapping τ_{t2}. Calculations for this model were done for every combination of these rates $(\tau_{t1},\tau_{rt1},\tau_{t2})$, where $\tau_{t1} \in (10\ ns,100\ ns,1\ \mu s)$, $\tau_{rt1} \in (10\ ns,100\ ns,1\ \mu s,10\ \mu s)$ and the $\tau_{t2} \in (10\ ns,100\ ns,1\ \mu s,10\ \mu s,100\ \mu s,1\ ms)$.

Model M3

The third model is devoted to the kinetics occurring from two separate trap states. We have considered two different trap types, radiative (R) and nonradiative (NR) ones. They can be independently occupied by electrons and are characterized by different trapping and detrapping rates. Transitions considered in model M3 are schematically presented in **fig. S6**. Each trap centre can be occupied by only one electron. R-centres are characterized by a fast trapping rate followed by possible radiative recombination of a trapped electron (similar to model **M1**). NR-centres are of non-emissive character and each electron is trapped for a longer time (similar to conventional charging model) to provide sustained charge off-balance. Only detrapping to a higher excited state or nonradiative decay are allowed for NR-centres. One may consider different physics behind these two types of traps. Radiative centres could be related to point defects, whereas nonradiative traps could originate from surface or ligand-related defects.

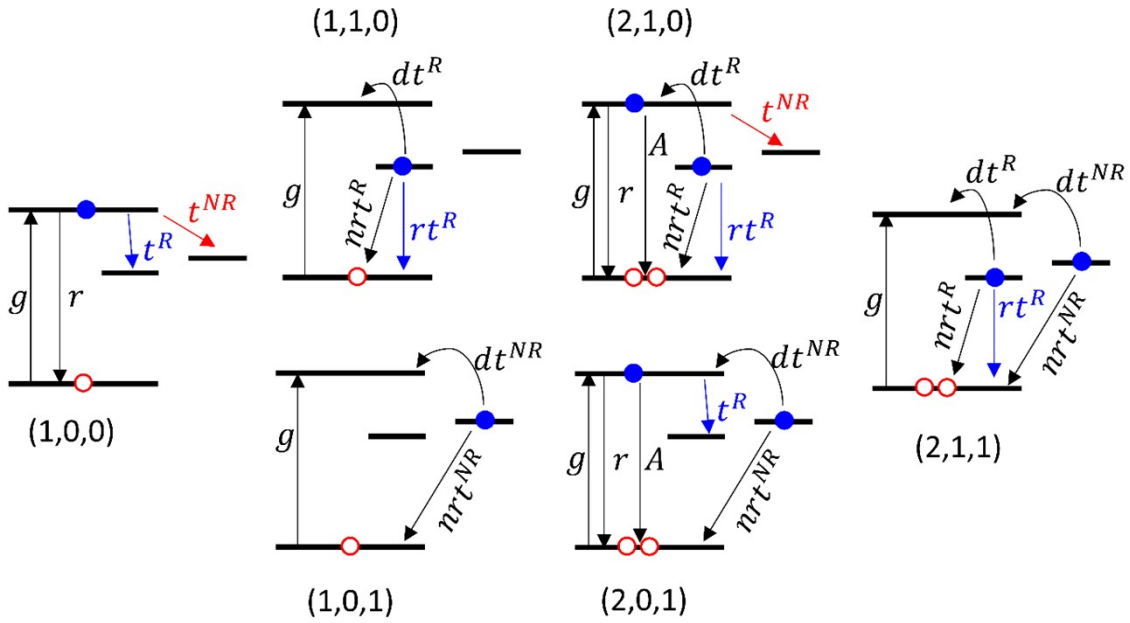

$r = 10\ ns$ $\quad dt^R = dt^{NR} = 100\ ms$ $\quad t^R = var.$ $\quad t^{NR} = var.$

$A = 1\ ns$ $\quad nrt^R = nrt^{NR} = 100\ ms$ $\quad rt^R = var.$

Figure S6. Simplified flow chart of electronic transitions comprised by model **M3.** This model is used to describe competitive interaction between radiative (superscript **R**) and non-radiative (superscript **NR**) trap centres. Rates common for all calculations: $\tau_r = 10\ ns$, $\tau_A = 1\ ns$, $\tau_{dt}^R = \tau_{dt}^{NR} = 100\ ms$, $\tau_{nrt}^R = \tau_{nrt}^{NR} = 100\ ms$ were noted in black. Rates varied in calculations were noted in blue and red. Filled blue circles represent electrons, while open red circles represent holes. The (i,j,k) indexing convention is shown for each state in parentheses.

This scheme also uses three parameters indexing to describe the QD state. The (i,j,k) indices are used, where i is the total number of excited electron-hole pairs, j is the number of occupied R-centres and k is the number of occupied NR-centres. We define $p = i$ and $n = i - j - k$ as the number of free holes and free electrons respectively. The indices $s^- = j$ and $z^- = k$ are the number of electrons trapped by radiative and nonradiative traps respectively. We arbitrary set the total number of radiative traps as $s = s^0 + s^- = 10$ and nonradiative traps as $z = z^0 + z^- = 5$.

Table S4. Rate equations for processes included in model M3.

Process		Shortcut	Rate equation
Generation		g	$\frac{I \cdot \sigma}{E_{ph}}$
Exciton radiative recombination		r	$k_r \cdot n \cdot p$
Charge trapping	R-centre	t^R	$k_r \cdot n \cdot p$
	NR-centre	t^{NR}	$k_t^R \cdot n \cdot s^0$
Charge detrapping	R-centre	dt^R	$k_t^{NR} \cdot n \cdot z^0$
	NR-centre	dt^{NR}	$k_{dt}^R \cdot s^-$
Nonradiative recombination from trap state	R-centre	nrt^R	$k_{dt}^{NR} \cdot z^-$
	NR-centre	nrt^{NR}	$k_{nrt}^R \cdot s^- \cdot p$
Radiative recombination from trap state	R-centre	rt^R	$k_{nrt}^{NR} \cdot z^- \cdot p$
	NR-centre	rt^{NR}	not allowed
Auger		A	$k_A \cdot n \cdot p^2$

Rate equations describing the rates of transitions of excited electrons to these traps as well as detrapping events are analogous to previous charging model and M1 model with slightly different definitions of electron and hole numbers (**tab. S4**). Detrapping rates for both traps were set to $\tau_{dt}^R = \tau_{dt}^{NR} = 100\ ms$ and were equal to nonradiative decay time constants $\tau_{nrt}^R = \tau_{nrt}^{NR} = 100\ ms$. These parameters were fixed and common for all calculations within this model. Radiative recombination from a NR-traps was not possible.

To examine the competitive influence of both traps on the photoluminescence from a single QD, the calculations for this model were done for every combination of rate constant $(\tau_t^R, \tau_{rt}^R, \tau_t^{NR})$.
These parameters were varied in ranges $\tau_t^R \in (10\ ns, 100\ ns, 1\ \mu s)$, $\tau_{rt}^R \in (10\ ns, 100\ ns, 1\ \mu s, 10\ \mu s)$ and the $\tau_t^{NR} \in (10\ ns, 100\ ns, 1\ \mu s, 10\ \mu s, 100\ \mu s, 1\ ms)$.

Section 5. Calculation results and discussion

Conventional charging model

Exciton recombination is the only source of emission from QD. Lifetime of excitonic emission is characterized by short lifetime of several tenths of nanoseconds.[6] For low generation rates under continuous excitation, where $k_r > g$, radiative recombination from single electron-hole pair dominates ($k_r = 10^8\ s^{-1}$) after excitation. Trapping of an excited electron is a low-probable process due to its slow rate ($k_t \in 10^2 - 10^4\ s^{-1}$) and it happens rarely every few bins. After trapping of an electron luminescence is rapidly quenched by very fast nonradiative Auger recombination ($k_A = 10^9\ s^{-1}$). ON/OFF switching results in well defined intensity levels corresponding to neutral exciton (bright state) and charged trion (dark state) emission observed in PL traces and FLID maps (**fig. S7**)

Ye and Searson[4] have calculated the effective trapping ($r_{t,eff}$) and detrapping ($r_{d,eff}$) rates considering all configurations in individual QD. For their charging model effective trapping rate is equal to $r_{t,eff} = sk_t g/k_r$ while effective detrapping is $r_{d,eff} = k_{dt} + k_{nrt}$. The increase of effective trapping rate either by nonradiative recombination or tunnelling of an electron back to the excited state reduces blinking behaviour and restores the ON state of a QD. Model blinking behaviour is reproduced when a ratio $r_{t,eff}/r_{d,eff}$ is in the range from 10^{-2} to 10^2 (**fig. S7**).

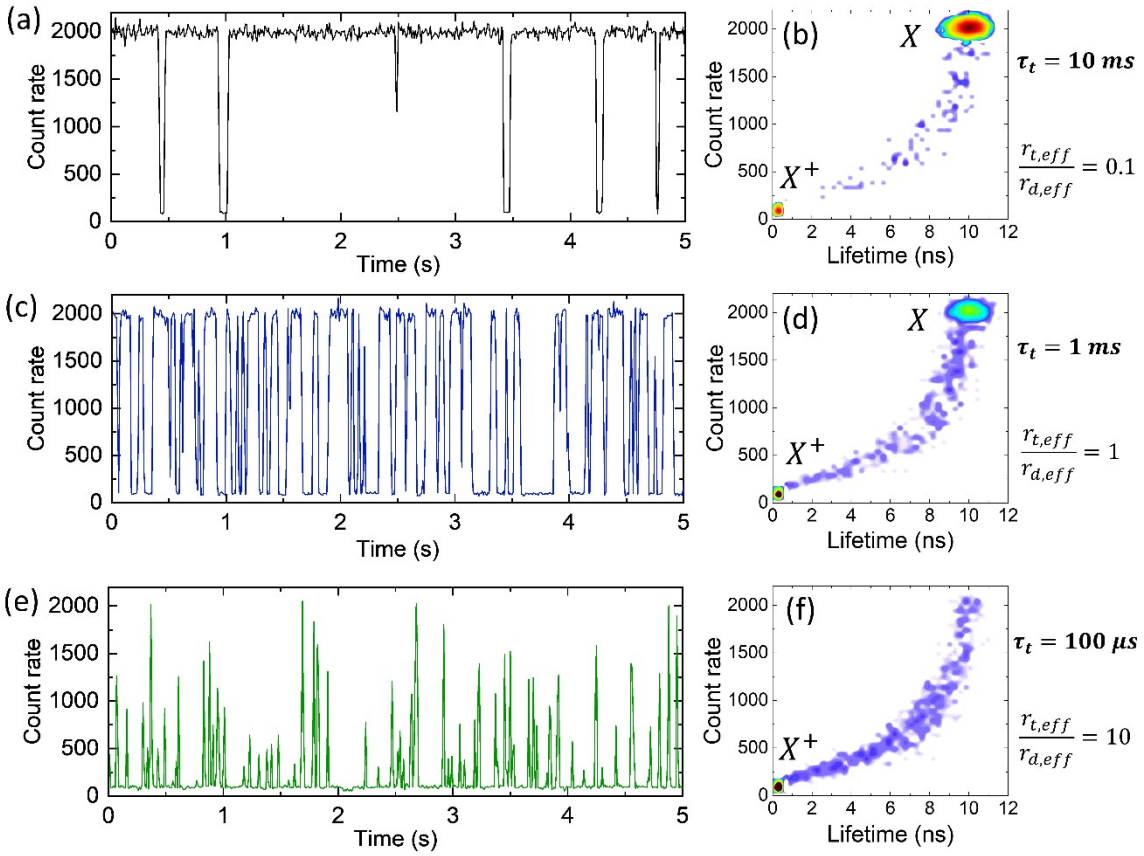

Figure S7. PL traces (a,c,e) and FLID maps (b,d,f) calculated for three values of trapping rate: (a,b) τ_t=10 ms, (c,d) τ_t=1 ms and (e,f) τ_t=100 μs. Nonradiative recombination rate was τ_{nrt}=100 ms. Other rates the same as in **fig. S3**. Count rate in photons/10 ms.

Long-lasting charge blocking is necessary to obtain dark state with near-zero emission intensity due to effective PL quenching via Auger processes. Efros and Rosen have considered very long charging with detrapping lifetime 0.8 s.[3] In all models presented in this work a lifetime of 0.1 s was sufficient to provide long-lasting stay of an electron in a trap. For slow trapping rate (τ_t=1 ms) and nonradiative recombination rate (τ_{nrt}≤ 100 μs) continuous bright state with maximum intensity was obtained (**fig. S8**). If trapping events are rare (i.e. occur once every few bins), any detrapping process faster than binning time (10 ms) will result in continuous bright state.

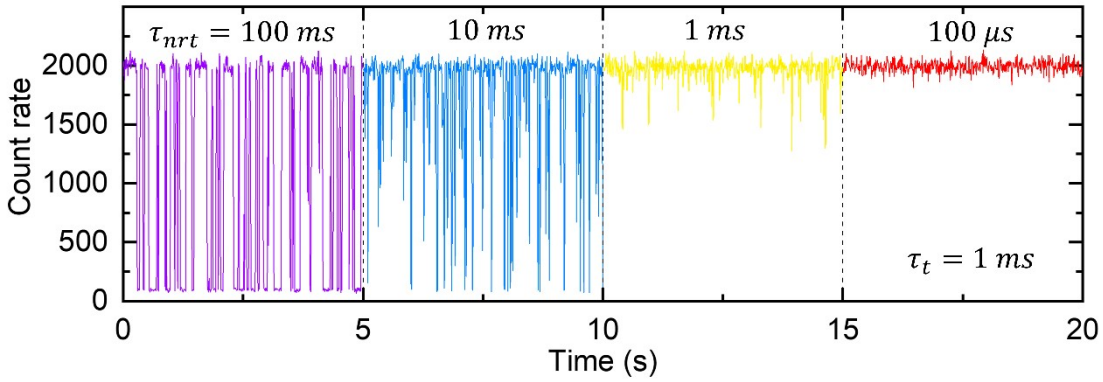

Figure S8. PL traces calculated with varying nonradiative recombination rate τ_{nrt} and fixed trapping rate τ_t=1 ms. Other parameters like in **fig. S3**. Count rate in photons/10 ms.

Considering fast trapping processes (τ_t≤1 μs) but slow release of trapped electrons, large charge off-balance can build up relatively quickly by simultaneous filling of several long-living traps. It will result in complete quenching of any emission from a QD and continuous dark state. On the other hand, slow trapping (τ_t>1 ms, once every few bins) followed by recombination faster than a binning time has almost no negative impact on the emission. QD remains in continuous bright state with maximal emission intensity. When effective trapping and detrapping rates are bath faster than binning time, the switching between ON and OFF states will occur multiple times within single bin resulting in continuous emission with intermediate intensity (**fig. S9** and **fig. S10**).

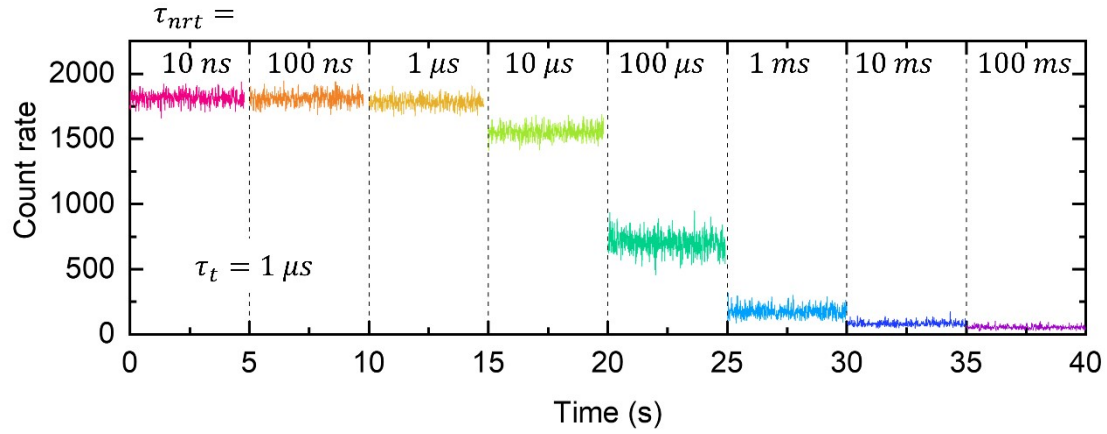

Figure S9. PL traces calculated with varying nonradiative recombination rate τ_{nrt} and fixed trapping rate τ_t=1 µs. Other parameters like in **fig. S3**. Count rate in photons/10 ms.

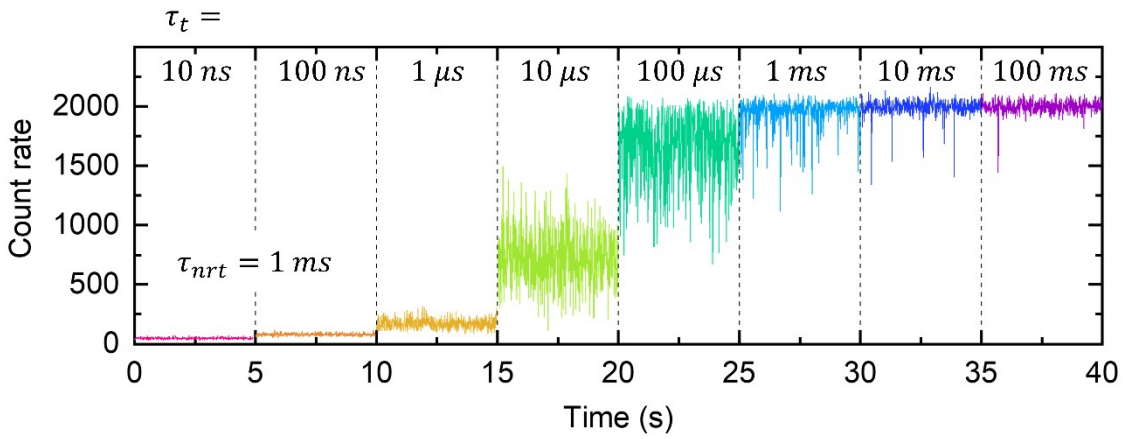

Figure S10. PL traces calculated with varying trapping rate τ_t and fixed nonradiative recombination rate τ_{nrt}=1 ms. Other parameters like in **fig. S3**. Count rate in photons/10 ms.

M1 model

In this model after generation one of two relaxation pathways takes place. Since excitonic recombination lifetime was fixed to $\tau_r = 10\ ns$, the share of a given relaxation pathway in a total emission depends on trapping lifetime τ_t and number of empty traps that can accept excited electron s_0. For τ_t=$10\ ns$ trapping of an excited electron is even more probable than radiative recombination (τ_r=$10\ ns$) with a hole, and that is due to the number of available trap states (s_0=10) compared to only one free hole in the valence band. In this case the total emission intensity occurs mostly from defect emission (90% of total emission intensity, **fig. S11 a-d**) and the excitonic emission is in the minority (10% of total emission). Slowing the trapping rate by one order of magnitude (τ_t=$100\ ns$) results in comparable rates of exciton emission and defect emission with equal participation of both emission mechanisms in the total emission intensity (50%/50%, **fig. S11 e-h**). Further slowing of the trapping rate to τ_t=$1\ \mu s$ results in 90% contribution of the exciton emission to the total intensity (**fig. S11 i-l**).

One may see, that for fast defect emission rates (τ_{rt}≤1 µs) Auger processes do not influence the emission. Trapped electron recombines radiatively before next generation event. However, for slower radiative recombination (τ_{rt}=10 µs) second generation may occur before recombination of previously trapped electron. Auger processes quench the emission and one may observe a decrease in the total emitted intensity, but no switching between distinct ON and OFF states. However, the ratio of the exciton emission to trap state emission is preserved (**fig. S11 d, h, i**).

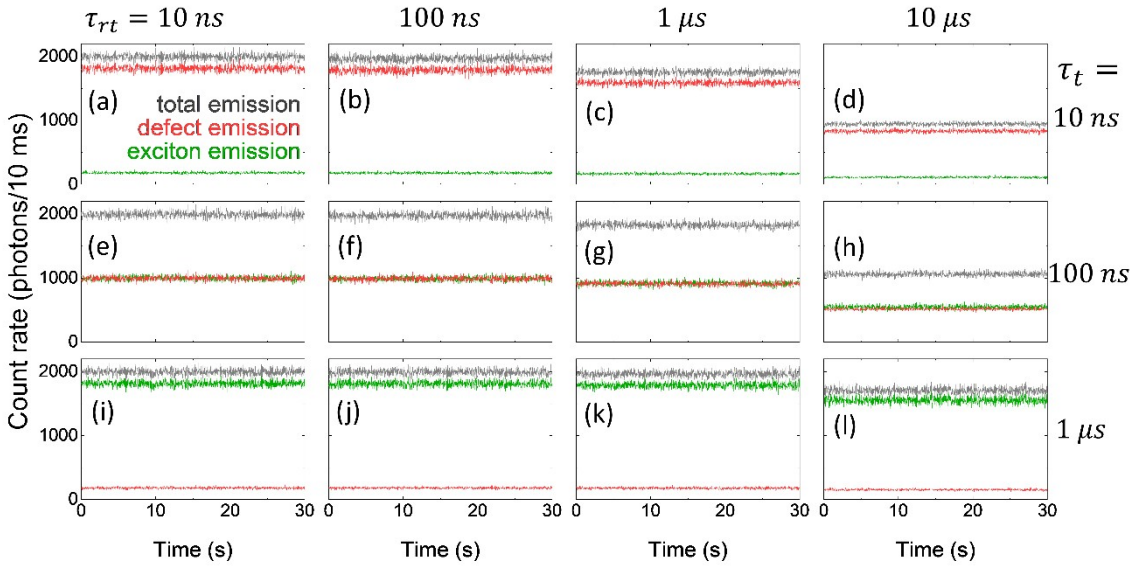

Figure S11. PL traces calculated within model M1 with varying trapping rate τ_t and defect radiative recombination rate τ_{rt}. Exciton, defect and total emission were plotted in green, red and black respectively. Other parameters like in **fig. S4**.

Blinking behaviour in model M1 can be restored only when rates of trapping and radiative recombination are lowered and **M1** model reduces to simple charging model (**fig. S10**, ESI). Considering slow trapping rate (τ_t=1 ms), radiative recombination of trapped electron is just another detrapping channel. It follows the rules deduced from reference charging model. Continuous bright state with maximum intensity is obtained for any radiative recombination rate faster than τ_{rt}=10 ms (**fig. S12**). One may notice that the number of photons emitted from a trap state is quite low and doesn't exceed 3 photons per 10 ms bin (**fig. S12**). This is well rationalized considering the low occupation rate of the trap state due to the relatively long time needed for an excited electron to be trapped i.e. τ_t=1 ms.

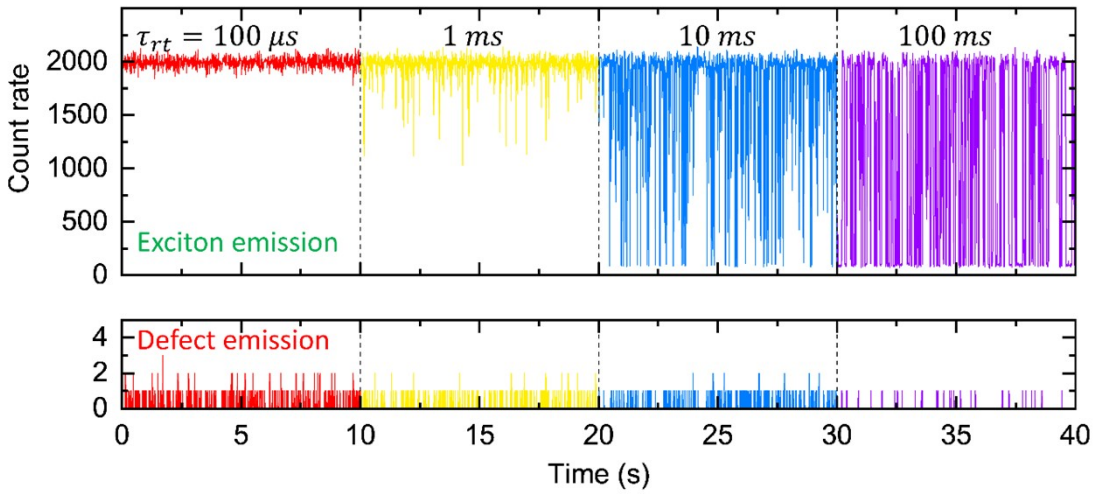

Figure S12. PL traces calculated within model M1 with fixed τ_t=1 ms, and with varying defect radiative recombination rate τ_{rt}. Top panel: exciton emission, bottom panel: defect emission. Count rate in photons/10 ms.

M2 model

Calculations within M2 model were done for every combination of $(\tau_{t1},\tau_{rt1},\tau_{t2})$ rates for wide range of values $\tau_{t1} \in (10\ ns, 100\ ns, 1\ \mu s)$, $\tau_{rt1} \in (10\ ns, 100\ ns, 1\ \mu s, 10\ \mu s)$ and $\tau_{t2} \in (10\ ns, 100\ ns, 1\ \mu s, 10\ \mu s, 100\ \mu s, 1\ ms)$. In such an approach, it is possible to find trends in the kinetics of the optical processes resulting from an interplay between two temporarily correlated trapping processes. PL traces of total emission for every calculation set are presented in **fig. S13, S14, S15**.

It was found, that the ratio of the defect emission to the excitonic emission follows the same trend as in the **M1** model and it depends only on the first electron trapping rate τ_{t1}. Assuming that the second electron trapping rate is slow ($\tau_{t2} \geq 10\ \mu s$), the **M2** model would reduce to the M1 model. In such a case, blinking is rarely observed and the bright state dominates the emission. For faster second electron trapping rates i.e. $\tau_{t2} \in (10\ ns, 100\ ns, 1\ \mu s)$ blinking is well pronounced. Dark states emerge more often for slower radiative recombination rates (τ_{rt1}) and for fast first electron trapping τ_{t1}. It is well rationalized that to get double-occupied traps, fast single-electron trap population as well as long occupation are necessary. For single charged trap centres, the radiative recombination rate is the only non-fixed detrapping parameter. Slowing down the radiative recombination rate to $\tau_{rt1} \in (1\ \mu s, 10\ \mu s)$ results in lower total emitted intensity due to the increasing value of the Auger processes. This effect is even more visible for faster first electron trapping (τ_{t1}=$10\ ns$), which is also consistent with results discussed for model **M1** (**fig. S11**). One may note that, for model **M2**, bright states dominate and dark states emerge in the form of thin peaks of lower intensity, but minimal intensity is not always reached. Dark states are short, and ON/OFF switching is rather fast. It may occur several times in every binning period (10 ms). Even for calculations where the bright state is greatly reduced and emission is in the form of thin peaks of about one bin duration, dark states are also short-living. Emission peaks are dense and not well separated. After second electron trapping, two holes remaining in QD's core promote very rapid Auger processes, due to quadratic scaling of Auger recombination rate with number of free holes ($k_A np^2$). However, effective detrapping is relatively faster than in conventional charging model. It is due to higher number of carriers (2 electrons and 2 holes) that participate in detrapping processes.

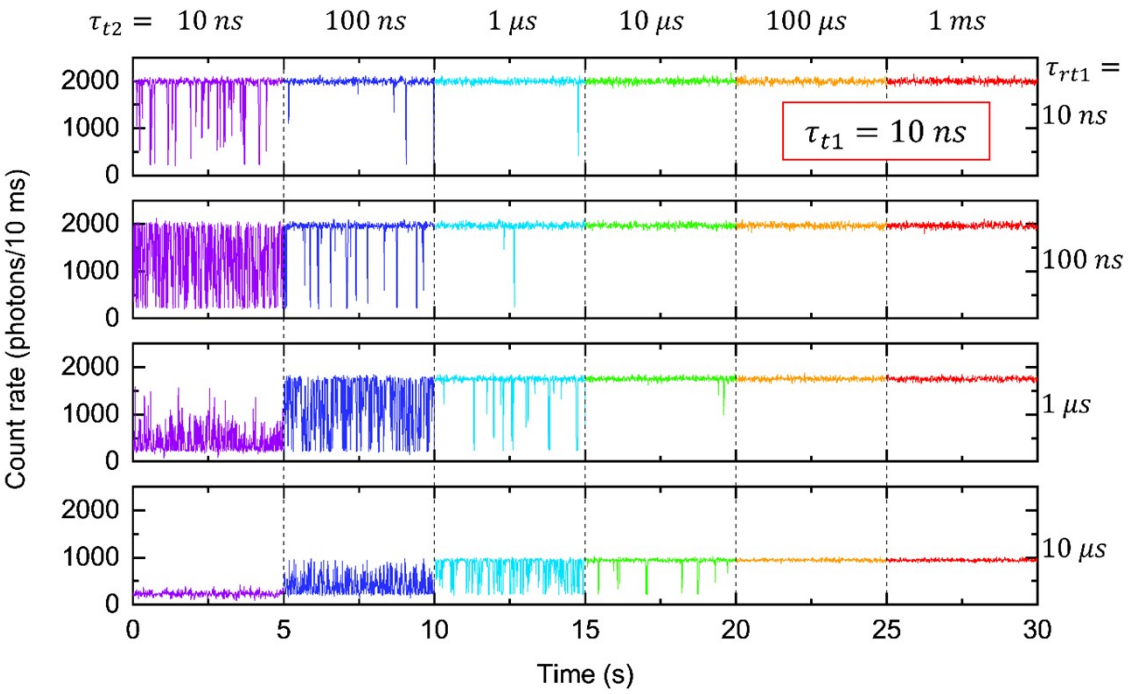

Figure S13. PL traces of total emission calculated within M2 model with fixed first electron trapping rate (τ_{t1}=10 ns) and varying single charged defect radiative recombination rate (τ_{rt1}) and second electron trapping rate (τ_{t2}).

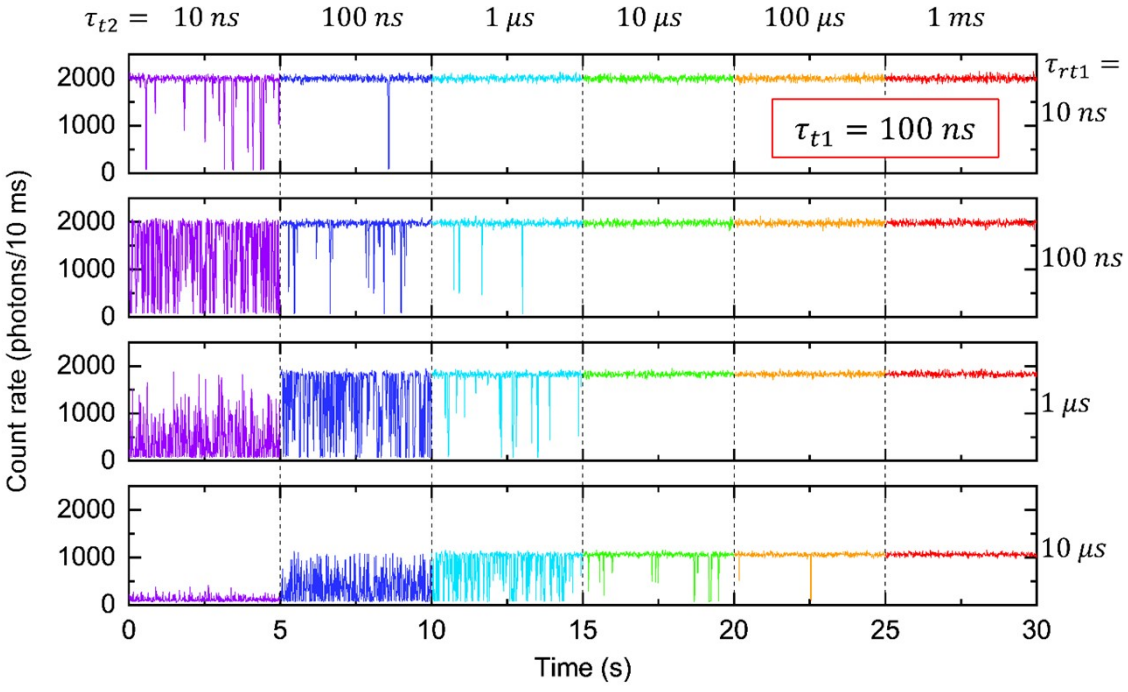

Figure S14. PL traces of total emission calculated within M2 model with fixed first electron trapping rate (τ_{t1}=100 ns) and varying single charged defect radiative recombination rate (τ_{rt1}) and second electron trapping rate (τ_{t2}).

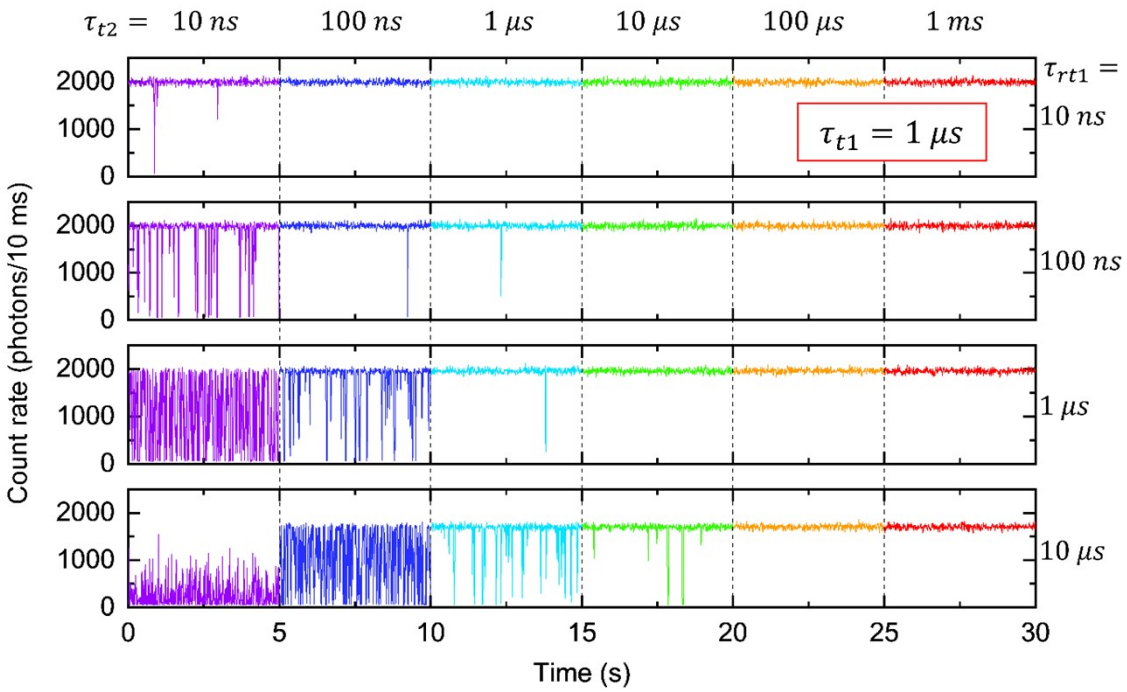

Figure S15. PL traces of total emission calculated within M2 model with fixed first electron trapping rate (τ_{t1}=1 μs) and varying single charged defect radiative recombination rate (τ_{rt1}) and second electron trapping rate (τ_{t2}).

M3 model

Similar to previous model, calculations within M3 model were done for every combination of $(\tau_t^R, \tau_{rt}^R, \tau_t^{NR})$ rates for wide range of values $\tau_t^R \in (10\ ns, 100\ ns, 1\ \mu s)$, $\tau_{rt}^R \in (10\ ns, 100\ ns, 1\ \mu s, 10\ \mu s)$ and $\tau_t^{NR} \in (10\ ns, 100\ ns, 1\ \mu s, 10\ \mu s, 100\ \mu s, 1\ ms)$. PL traces of total emission for every calculation set are presented in **fig. S16, S17, S18**. In such an approach, it is possible to find trends in the kinetics of the optical processes resulting from an interplay between two independent trapping channels.

Once again, the defect to exciton emission ratio follows the trend observed in M1 model and depends only on the radiative centre trapping rate. Assuming fast trapping to nonradiative centres $\tau_t^{NR} \in (10\ ns, 100\ ns, 1\ \mu s)$, the excited electron can be trapped with a probability similar to the radiative centre trapping. Fast trapping and long stay of an electron in the NR-centre provides a long-lasting strong charge imbalance and promotes nonradiative Auger recombination. Therefore, the emission from the QD for $\tau_t^{NR} \leq 1\ \mu s$ is almost completely quenched. Slowing down the trapping rate by NR-centres ($\tau_t^{NR} \geq 10\ \mu s$) results in restoration of the bright state. This is also accompanied by well pronounced blinking behaviour. Unlike model **M2,** the well outlined OFF states with typical length of several bin times can be observed. The OFF state is, however, associated with a non-zero emission intensity similar to the experimental PL traces observed for CIS QDs (**fig. S1**). This residual emission is associated with defect emission after population of non-emissive traps. Its minimal intensity emitted in the OFF state depends on the R-centres trapping rate and reaches almost 25% of maximal total emission intensity (500 photons per bin) for fastest trapping rate $\tau_t^R = 10\ ns$. Slower trapping by radiative centres $\tau_t^R \in (100\ ns, 1\ \mu s)$ results in lower intensity emitted in the OFF state: about 8% and 5% of maximal total intensity (150 and 90 photons respectively). Similar to the **M1** model, only one occupied NR-trap is sufficient for the occurrence of blinking behaviour. However, for fast trapping by NR-centres it is

possible to populate more than one centre resulting in further stepwise lowering of the emission level during the OFF state. Such behaviour is particularly visible for τ_t^{NR}=10 μs.

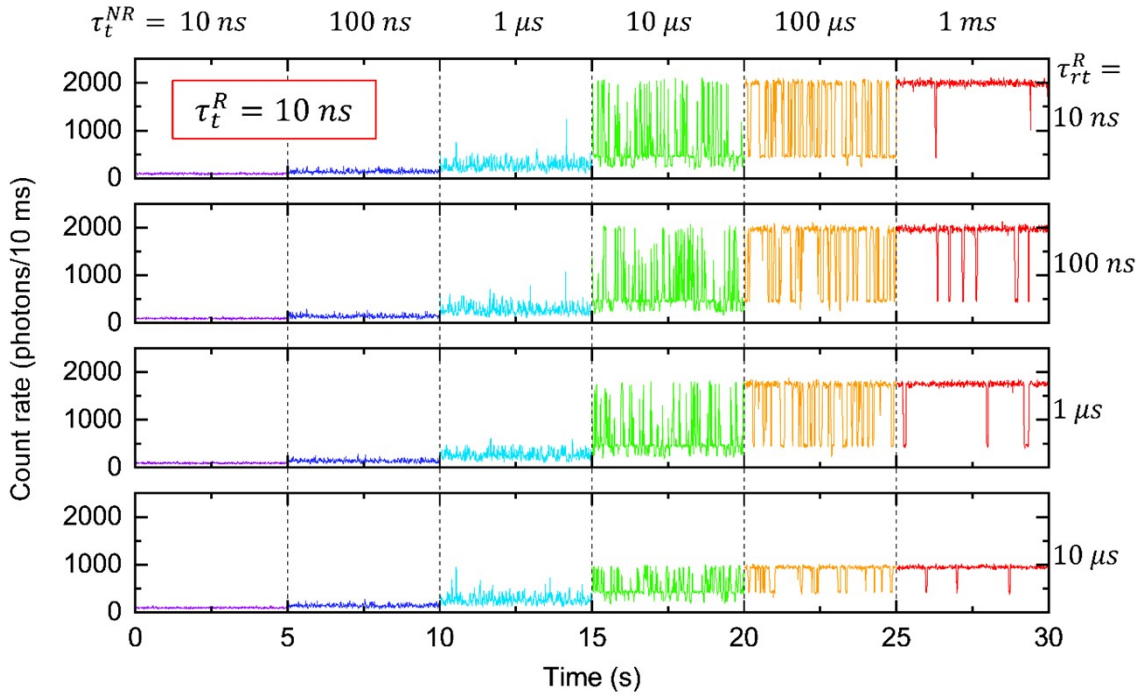

Figure S16. PL traces of total emission calculated within M3 model with fixed radiative centres trapping rate (τ_t^R=10 ns) and varying defect radiative recombination rate (τ_{rt}^R) and nonradiative centres trapping rate (τ_t^{NR}).

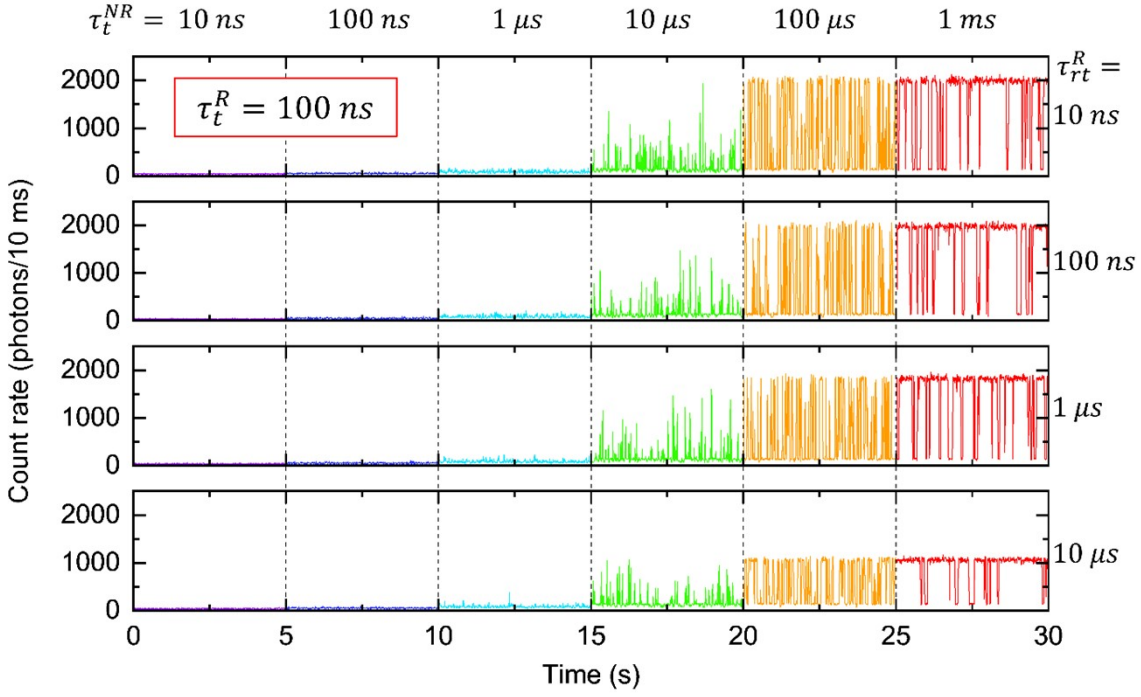

Figure S17. PL traces of total emission calculated within M3 model with fixed radiative centres trapping rate (τ_t^R=100 ns) and varying defect radiative recombination rate (τ_{rt}^R) and nonradiative centres trapping rate (τ_t^{NR}).

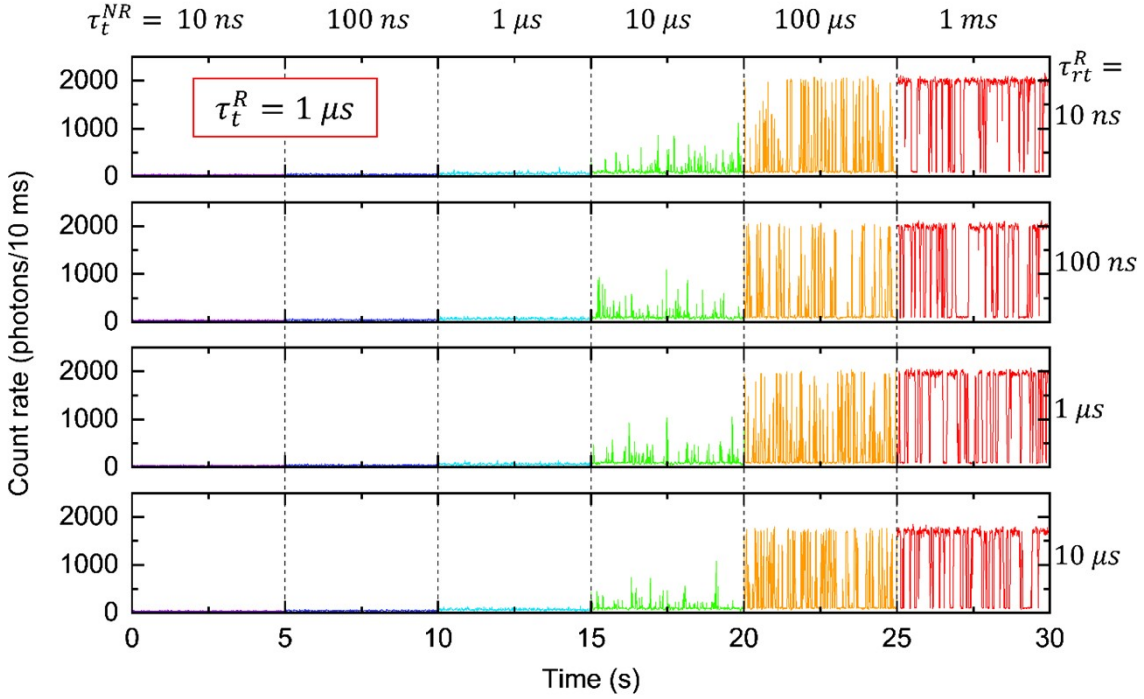

Figure S18. PL traces of total emission calculated within M3 model with fixed radiative centres trapping rate (τ^R_t=1 μs) and varying defect radiative recombination rate (τ^R_{rt}) and nonradiative centres trapping rate (τ^{NR}_t).

References

1 W. M. Young and E. W. Elcock, *Proc. Phys. Soc.*, 1966, **89**, 735–746.

2 A. B. Bortz, M. H. Kalos and J. L. Lebowitz, *J. Comput. Phys.*, 1975, **17**, 10–18.

3 A. L. Efros and M. Rosen, *Phys. Rev. Lett.*, 1997, **78**, 1110–1113.

4 M. Ye and P. C. Searson, *Phys. Rev. B - Condens. Matter Mater. Phys.*, 2011, **84**, 125317.

5 X. Hou, J. Kang, H. Qin, X. Chen, J. Ma, J. Zhou, L. Chen, L. Wang, L. W. Wang and X. Peng, *Nat. Commun.*, 2019, **10**, 1750.

6 M. Califano, A. Franceschetti and A. Zunger, *Nano Lett.*, 2005, **5**, 2360–2364.